DALTON
FULL PAPER

Synthesis and structural studies on polymeric assemblies derived from antimony(III) halide complexes with bi- and tri-dentate and macrocyclic thio- and seleno-ether ligands

Andrew J. Barton, Nicholas J. Hill, William Levason and Gillian Reid

Department of Chemistry, University of Southampton, Highfield, Southampton, UK SO17 1BJ

Received 23rd January 2001, Accepted 4th April 2001
First published as an Advance Article on the web 24th April 2001

SbX_3 (X = Cl, Br or in some cases I) reacts with one molar equivalent of L [L = $MeS(CH_2)_2SMe$, $MeS(CH_2)_3SMe$, $MeSe(CH_2)_2SeMe$, $MeC(CH_2SMe)_3$, $MeC(CH_2SeMe)_3$, [12]aneS_4 (1,4,7,10-tetrathiacyclododecane), [14]aneS_4 (1,4,8,11-tetrathiacyclotetradecane), [16]aneS_4 (1,5,9,13-tetrathiacyclohexadecane), [8]aneSe_2 (1,5-diselenacyclooctane) or [16]aneSe_4 (1,5,9,13-tetraselenacyclohexadecane)] in anhydrous CH_2Cl_2, MeCN or thf solution to afford colourless to red-orange powdered solids involving a 1 : 1 Sb : L ratio in most cases, and occasionally a 2 : 1 Sb : L ratio. The crystal structures of [$SbCl_3\{MeS(CH_2)_2SMe\}$], [$(SbBr_3)_2$([14]aneS_4)], [$SbCl_3\{MeC(CH_2SMe)_3\}$], [SbI_3-$\{MeC(CH_2SMe)_3\}$] and [$SbBr_3\{MeC(CH_2SeMe)_3\}$] all exhibit infinite one- or three-dimensional networks which are assembled from distorted five or six coordinate Sb(III) with primary Sb–X bonding, secondary Sb–S or Sb–Se interactions and retention of the pyramidal SbX_3 unit found in the parent halides. The structures of these compounds are discussed in terms of the bonding model used by others for antimony phosphine complexes. They are also compared with the structures of other reported thioether complexes of Sb(III), and with their Bi(III) analogues.

Introduction

The coordination chemistry of the p-block elements with thio-, seleno- or telluro-ether ligands has been relatively little explored. We have recently described the preparations and structures of a series of multidentate and macrocyclic thio- and seleno-ether complexes with Bi(III) halides. These species exhibit a surprisingly diverse array of structural motifs, including for example, an infinite three-dimensional array involving pseudo cubane Bi_4Cl_4 units with bridging dithioethers, and one-dimensional ladders involving exocyclic coordination of macrocyclic selenoethers.[1–3] We have turned our attention to Sb(III) species in an attempt to probe the effect of moving from elements which are essentially metallic in nature to the metalloids. We recently communicated our initial findings, *viz* the first examples of Sb(III) selenoether complexes, [$(SbBr_3)_2$([16]aneSe_4)] which adopts a two-dimensional network with exocyclic macrocycle coordination giving a distorted square pyramidal environment at Sb(III), and [$SbCl_3\{MeSe(CH_2)_3SeMe\}$] which adopts an infinite one-dimensional chain with a distorted octahedral coordination environment at Sb(III).[4] Crown ether complexes with SbX_3 all show a monomeric SbX_3 unit capped by the macrocyclic ligand, *e.g.* [$SbCl_3$(15-crown-5)] which shows all five ether O atoms bonded to a pyramidal $SbCl_3$ unit in a half sandwich structure.[5] Other structurally characterised examples of Sb(III) complexes containing crown ethers include [$SbCl_3$(12-crown-4)] and [$SbCl_3$(18-crown-6)].[6,7] In all of these compounds the $SbCl_3$ units retain the pyramidal geometry of the parent halide.[8] The Sb–O distances are *ca.* 0.6 Å longer than the Sb–Cl bonds. Recent reports have also provided crystal structures for the dinuclear compounds [$(SbX_3)_2$(dibenzo-24-crown-8)] (X = Cl or Br).[9]

Studies on thioether crown complexes of Sb(III) have also confirmed that the effect of the lone pair is to leave the geometry of the $SbCl_3$ unit essentially unchanged following coordination of the macrocycle. The complexes [$SbCl_3$([9]aneS_3)], [$(SbCl_3)_2$([18]aneS_6)] and [SbI_3([9]aneS_3)] have been structurally characterised.[10,11] In both of the trichloride complexes, the Sb atoms are weakly coordinated to the sulfur atoms with Sb–S distances in the range 2.968(2)–3.460(3) Å. The Sb–Cl distances in [$SbCl_3$([9]aneS_3)] [2.374(3)–2.451(3) Å] and [$(SbCl_3)_2$([18]aneS_6)] [2.381(3)–2.471(2) Å] are similar to those of the pyramidal core unit in crystalline $SbCl_3$ itself [2.340(2) and 2.368(1) Å].[8] In [$(SbCl_3)_2$([18]aneS_6)] the Sb centres are six coordinate with each of the three crown sulfur atoms *trans* to a chlorine atom in an irregular *fac*-octahedral array. One of the sulfur atoms is more distant from the metal centre than the other two. A similar [2 + 1] Sb–S bonding mode has been noted in [$SbCl_3$-$(EtNHCSCSNHEt)_{1.5}$][12] and [$SbCl_3$(1,4-dithiacycloheptane)].[13] In [$SbCl_3$([9]aneS_3)] the metal centres adopt a completely different stereochemistry giving an infinite chain structure. The Sb–S distances are quite similar to the Sb–O distances in the $SbCl_3$ crown ether complexes discussed above. SbI_3 forms a 1 : 1 adduct with [9]aneS_3. The crystal structure exhibits a discrete molecular structure with a distorted octahedral coordination at Sb(III) and there is no significant stereochemical influence of the Sb(III) lone pair. [$SbBr_3\{MeS(CH_2)_3SMe\}$] adopts a two-dimensional sheet with a distorted octahedral S_3Br_3 donor set at Sb (Sb–S = 3.155(5)–3.291(5) Å).[4]

In this paper we describe the results of an investigation into the reaction of Sb(III) halides with a range of bi- and tri-dentate and macrocyclic Group 16 ligands. The effects of changing halide are studied, and comparisons are made with Bi(III) halide compounds described previously.

Results and discussion

Reaction of SbX_3 (X = Cl, Br or in some cases I) with one molar equivalent of L [L = $MeS(CH_2)_2SMe$, $MeS(CH_2)_3SMe$, $MeSe(CH_2)_2SeMe$, $MeC(CH_2SMe)_3$, $MeC(CH_2SeMe)_3$, [12]aneS_4 (1,4,7,10-tetrathiacyclododecane), [14]aneS_4 (1,4,8,11-tetrathiacyclotetradecane), [16]aneS_4 (1,5,9,13-tetrathiacyclohexadecane), [8]aneSe_2 (1,5-diselenacyclooctane) or [16]aneSe_4 (1,5,9,13-tetraselenacyclohexadecane)] in anhydrous CH_2Cl_2, MeCN or thf solution affords colourless to red-orange solids which were isolated in moderate to good yield by filtration *in vacuo*. The majority of the products have empirical formula

DOI: 10.1039/b100782n

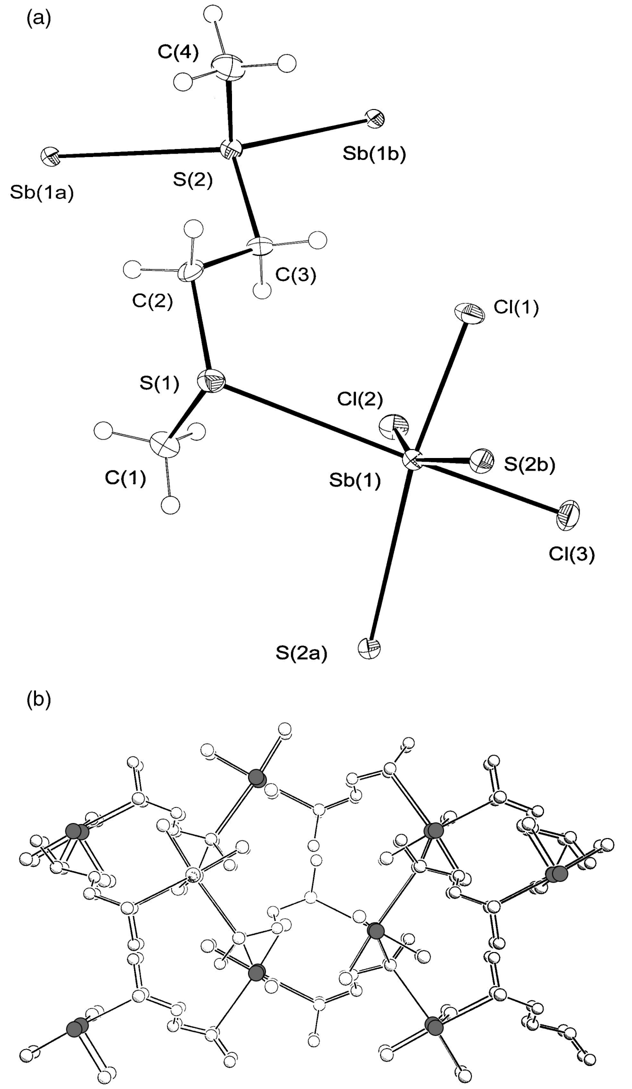

Fig. 1 a) View of the asymmetric unit of [SbCl$_3${MeS(CH$_2$)$_2$SMe}] with numbering scheme adopted and nearest symmetry related neighbours. Atoms marked (a) are related by $-x$, $\frac{1}{2}+y$, $\frac{1}{2}-z$, while atoms marked (b) are related by $\frac{1}{2}+x$, $\frac{1}{2}-y$, $-z$. Ellipsoids are drawn at the 40% probability level. b) View of the infinite three-dimensional lattice generated by symmetry expansion. Sb atoms are shaded.

Table 1 Selected bond lengths (Å) and angles (°) for [SbCl$_3${MeS(CH$_2$)$_2$SMe}]

Sb(1)–Cl(1)	2.384(2)	Sb(1)–S(1)	3.170(2)
Sb(1)–Cl(2)	2.411(2)	Sb(1)–S(2a)	3.294(2)
Sb(1)–Cl(3)	2.428(2)	Sb(1)–S(2b)	3.094(2)
Cl(1)–Sb(1)–Cl(2)	90.57(8)	Cl(2)–Sb(1)–S(2b)	164.20(7)
Cl(1)–Sb(1)–Cl(3)	91.02(7)	Cl(3)–Sb(1)–S(1)	176.89(3)
Cl(1)–Sb(1)–S(1)	86.69(6)	Cl(3)–Sb(1)–S(2a)	80.62(7)
Cl(1)–Sb(1)–S(2a)	164.23(7)	Cl(3)–Sb(1)–S(2b)	80.24(7)
Cl(1)–Sb(1)–S(2b)	74.73(7)	S(1)–Sb(1)–S(2a)	102.10(3)
Cl(2)–Sb(1)–Cl(3)	94.54(8)	S(1)–Sb(1)–S(2b)	97.12(6)
Cl(2)–Sb(1)–S(1)	87.58(7)	S(2a)–Sb(1)–S(2b)	116.47(2)
Cl(2)–Sb(1)–S(2a)	76.91(7)	Sb(1a)–S(2)–Sb(1b)	108.88(7)

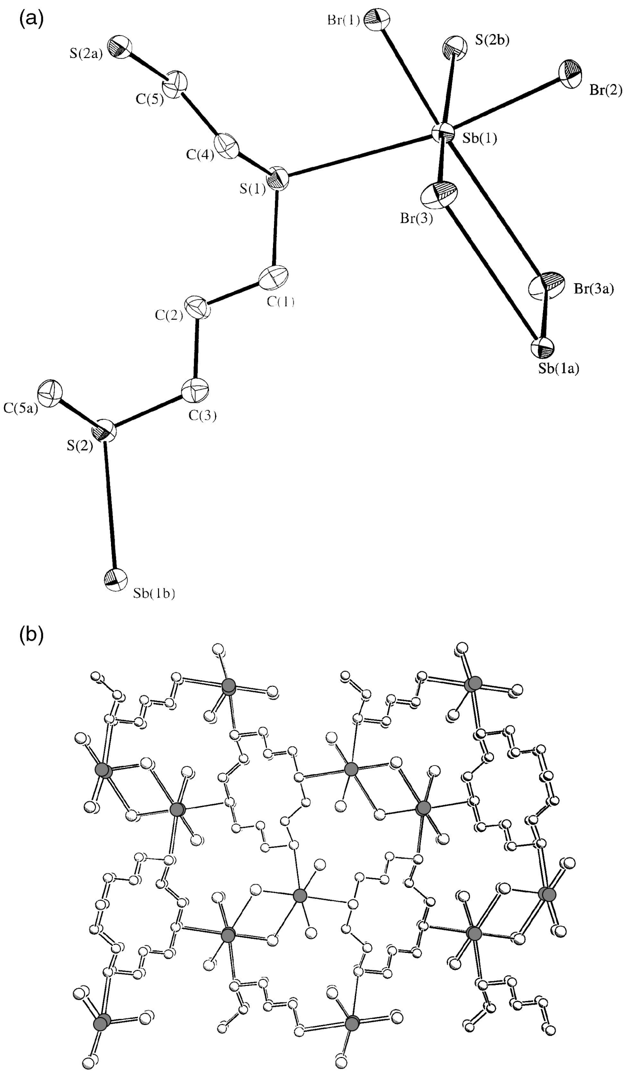

Fig. 2 a) View of the asymmetric unit of [(SbBr$_3$)$_2$([14]aneS$_4$)] with numbering scheme adopted and nearest symmetry related neighbours. Atoms marked (a) are related by $-x$, $-y$, $-z$, while those marked (b) are related by $\frac{1}{2}-x$, $\frac{1}{2}+y$, $\frac{1}{2}-z$. Ellipsoids are drawn at the 40% probability level. b) View of the three-dimensional [(SbBr$_3$)$_2$([14]aneS$_4$)] network generated by symmetry expansion (H atoms are omitted for clarity). Sb atoms are shaded.

Table 2 Selected bond lengths (Å) and angles (°) for [(SbBr$_3$)$_2$([14]aneS$_4$)]

Sb(1)–Br(1)	2.535(2)	Sb(1)–Br(3a)	3.497(2)
Sb(1)–Br(2)	2.548(2)	Sb(1)–S(1)	3.143(4)
Sb(1)–Br(3)	2.609(2)	Sb(1)–S(2b)	2.954(3)
Br(1)–Sb(1)–Br(2)	92.23(7)	Br(2)–Sb(1)–S(2b)	80.68(8)
Br(1)–Sb(1)–Br(3)	93.02(6)	Br(3)–Sb(1)–Br(3a)	84.99(6)
Br(1)–Sb(1)–Br(3a)	175.56(6)	Br(3)–Sb(1)–S(1)	88.79(8)
Br(1)–Sb(1)–S(1)	76.60(9)	Br(3)–Sb(1)–S(2b)	173.68(8)
Br(1)–Sb(1)–S(2b)	83.00(8)	S(1)–Sb(1)–S(2b)	95.21(9)
Br(2)–Sb(1)–Br(3)	94.62(6)	Br(3a)–Sb(1)–S(1)	105.30(8)
Br(2)–Sb(1)–Br(3a)	83.99(6)	Br(3a)–Sb(1)–S(2)	98.62(7)
Br(2)–Sb(1)–S(1)	170.38(8)	Sb(1)–Br(3)–Sb(1a)	95.01(6)

SbX$_3$(L), although in a few cases only the 2 : 1 M : L species (SbX$_3$)$_2$(L) were obtained. Similar observations were made for Bi(III) complexes of these ligands.[2,3] Reaction of SbCl$_3$ with MeSe(CH$_2$)$_2$SeMe yielded an orange oil, but we were unable to isolate a solid from this. Similar reactions with SbF$_3$ resulted only in re-isolation of SbF$_3$. Due to the moisture sensitivity of the Sb(III) halides, all reactions were carried out under an atmosphere of dry nitrogen using standard Schlenk techniques. All complexes were stored in a nitrogen purged dry-box. The thioether species are rather more stable as powdered solids under these conditions than the selenoether species which tend to decompose and darken over a period of a week or so. Satisfactory microanalyses were recorded for all freshly prepared solids. The IR spectra show the presence of the Group 16 donor ligand and, in the case of the chloro species, several peaks in the range *ca.* 300–230 cm^{-1} assigned to Sb–Cl stretching vibrations. The poor solubility of the complexes in non-coordinating solvents such as CH_2Cl_2 and $CHCl_3$ meant that NMR spectroscopy did not provide any useful information. Some of the complexes are sufficiently soluble in chlorocarbon solvents to permit room temperature ^{1}H NMR spectroscopic studies, however the spectra show resonances only a little shifted from 'free' ligand, with no evidence of different stereoisomers. The lack of structural information from the spectroscopic studies necessitated the use of X-ray crystallography to elucidate the structural features of the complexes.

X-Ray crystallography

Crystals of $[SbCl_3\{MeS(CH_2)_2SMe\}]$ were obtained by slow evaporation from an MeCN solution of the compound. The structure shows (Fig. 1, Table 1) a distorted octahedral coordination environment at Sb derived from three mutually *fac* terminal Cl's and three S atoms from different dithioethers, one terminal [S(1)] and two μ-bridging [S(2a) and S(2b)] which utilise both lone pairs of electrons to coordinate to different Sb centres. On each dithioether the second S atom coordinates to an adjacent Sb centre generating an infinite three-dimensional network. The Sb–S bond distances are in the range 3.094(2)–3.294(2) Å, indicating secondary interactions, while the Sb–Cl distances [2.384(2)–2.428(2) Å] are similar to those in the parent $SbCl_3$.[8] These bond distances are comparable with those reported for the other known $SbCl_3$/thioether complexes (above).[10,11,13,14] The structure of this species contrasts with that of $[BiCl_3\{MeS(CH_2)_2SMe\}_2]$, the product obtained from reaction of $BiCl_3$ with $MeS(CH_2)_2SMe$. This bismuth complex adopts a discrete molecular structure derived from a $BiCl_3$ fragment coordinated to two chelating dithioether ligands, giving a distorted pentagonal bipyramidal stereochemistry.[2]

The structure of the macrocyclic thioether species $[(SbBr_3)_2([14]aneS_4)]$ also adopts an infinite coordination network, although in this case the structure extends in all three dimensions. The repeat units consists of very weakly associated, asymmetric $Sb_2Br_6S_4$ edge-shared bioctahedra (Fig. 2, Table 2). The Sb atoms are coordinated to two terminal Br atoms and two μ-bridging Br atoms [Sb(1)–Br(3) = 2.609(2), Sb(1)–Br(3a) = 3.497(2) Å], with two terminal, mutually *cis* S atoms from distinct dithioethers completing the octahedron. Each $[14]aneS_4$ unit contributes one sulfur donor atom per antimony, bridging four separate antimony atoms in total. The Sb–S and Sb–Br bond distances show a similar pattern to those discussed above. This network structure contrasts with those reported for SbX_3 complexes with $[9]aneS_3$ and $[18]aneS_6$. These structural differences may be due to the different macrocyclic and chelate ring sizes available. Thus both $[9]aneS_3$ and $[18]aneS_6$ give the energetically favoured five-membered chelate rings both on Sb(III) and Bi(III), whereas $[14]aneS_4$ can give both five- and six-membered chelate rings, while coordination of two adjacent Se atoms in $[16]aneSe_4$ can only give the less stable six-membered chelate ring. Since the M–S and M–Se interactions are weak in these compounds, the chelate effect may be relatively important in determining the structures. The solubilities of the species may also play a significant role.

Surprisingly, the structures obtained for the three compounds $[SbCl_3\{MeC(CH_2SMe)_3\}]$, $[SbBr_3\{MeC(CH_2SeMe)_3\}]$ and $[SbI_3\{MeC(CH_2SMe)_3\}]$ exhibit quite different structural motifs for relatively small alterations in Group 16 ligand or halogen.

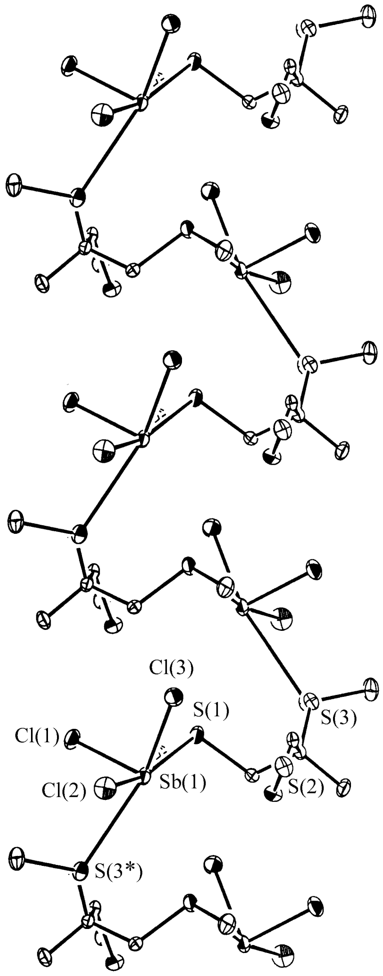

Fig. 3 View of part of the chain structure of $[SbCl_3\{MeC(CH_2SMe)_3\}]$ with numbering scheme adopted. Atoms marked (*) are related by $\frac{1}{2} - x, -y, \frac{1}{2} + z$. Ellipsoids are drawn at the 40% probability level and H atoms are omitted for clarity.

Table 3 Selected bond lengths (Å) and angles (°) for $[SbCl_3\{MeC(CH_2SMe)_3\}]$

Sb(1)–Cl(1)	2.393(2)	Sb(1)–S(1)	3.174(2)
Sb(1)–Cl(2)	2.407(2)	Sb(1)–S(3*)	3.108(2)
Sb(1)–Cl(3)	2.397(2)		
Cl(1)–Sb(1)–Cl(2)	95.54(6)	Cl(2)–Sb(1)–S(1)	167.27(6)
Cl(1)–Sb(1)–Cl(3)	91.85(6)	Cl(2)–Sb(1)–S(3*)	77.27(6)
Cl(1)–Sb(1)–S(1)	81.32(5)	Cl(3)–Sb(1)–S(1)	79.01(6)
Cl(1)–Sb(1)–S(3*)	80.84(5)	Cl(3)–Sb(1)–S(3*)	163.48(5)
Cl(2)–Sb(1)–Cl(3)	88.80(7)	S(1)–Sb(1)–S(3*)	114.11(4)

Crystals of $[SbCl_3\{MeC(CH_2SMe)_3\}]$ show (Fig. 3, Table 3) essentially five coordinate Sb(III) centres forming an infinite one-dimensional structure assembled from linking of these units by bridging $MeC(CH_2SMe)_3$ ligands. Each metal centre coordinates to a single sulfur atom from each of two different thioether ligands, giving a distorted square pyramidal geometry. The S atoms occupy mutually *cis* coordination sites at Sb. Each trithioether therefore functions as a μ-bridging ligand. The remaining S atom, S(2), may be considered to be very weakly associated with Sb(1) $\cdots$ S(2) = 3.462(2) Å. The infinitely repeating motif also retains some of the characteristics of the parent halide with bond lengths again indicative of primary Sb–Cl bonds [2.393(2)–2.407(2) Å] and weak, secondary Sb–S interactions [Sb(1)–S(1) 3.174(2), Sb(1)–S(3*) 3.108(2) Å]. For comparison, secondary Bi–S interactions in $BiCl_3$ complexes involving thioether ligands are also *ca.* 3.1 Å.[1,2,10,15]

Crystals were also obtained for the 1 : 1 reaction of SbI_3 with the tripodal thioether ligand, $MeC(CH_2SMe)_3$, in MeCN, although the actual crystal quality was rather poor and hence the final structure determination was of modest quality. The

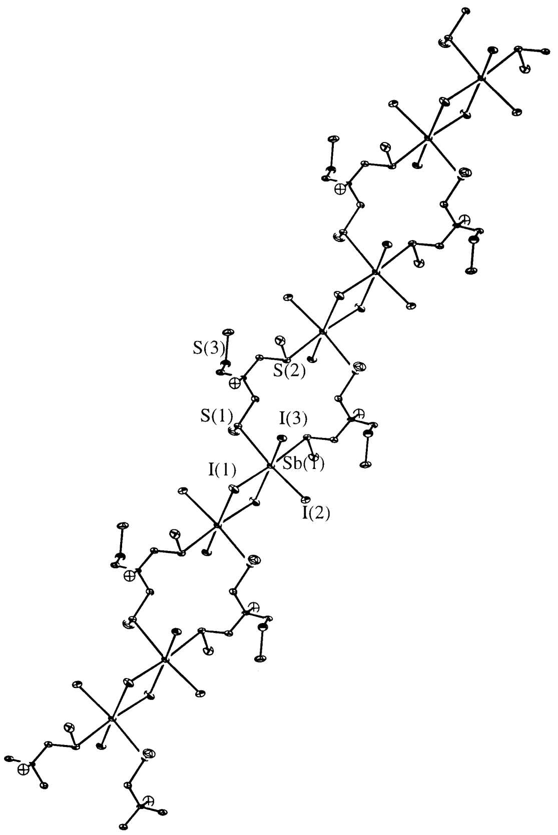

Fig. 4 View of part of the chain structure of [$\mathrm{SbI_3\{MeC(CH_2SMe)_3\}}$] with numbering scheme adopted. Atoms marked (*) are related by $-x$, $-y$, $-z$. Ellipsoids are drawn at the 40% probability level and H atoms are omitted for clarity.

Table 4 Selected bond lengths (Å) and angles (°) for [$\mathrm{SbI_3\{MeC(CH_2SMe)_3\}}$]

Sb(1)–I(1)	2.861(2)	Sb(1)–I(3)	2.771(2)
Sb(1)–I(1*)	3.516(2)	Sb(1)–S(1)	3.021(6)
Sb(1)–I(2)	2.847(2)	Sb(1)–S(2)	2.973(6)

Sb(1)–I(1)–Sb(1*)	94.95(6)	I(1)–Sb(1)–S(1*)	96.5(1)
I(1)–Sb(1)–I(1*)	85.05(6)	I(1)–Sb(1)–S(2*)	97.8(1)
I(1)–Sb(1)–I(2)	95.16(7)	I(2)–Sb(1)–I(3)	94.65(7)
I(1)–Sb(1)–I(3)	92.35(7)	I(2)–Sb(1)–S(1)	174.0(1)
I(1)–Sb(1)–S(1)	90.6(1)	I(2)–Sb(1)–S(2)	89.1(1)
I(1)–Sb(1)–S(2)	175.0(1)	I(3)–Sb(1)–S(1)	83.5(1)
I(1)–Sb(1)–I(2*)	85.61(6)	I(3)–Sb(1)–S(2)	84.8(1)
I(1)–Sb(1)–I(3*)	177.39(7)	S(1)–Sb(1)–S(2)	85.0(2)

structure determined for this example (Fig. 4, Table 4) illustrates that the subtle change of halogen from chlorine to iodine has a significant effect upon the structure adopted. Instead of five coordinate Sb(III) centres (chloro species) we now observe a six coordinate antimony. These results are consistent with reduced lone pair activity with the heavier iodide complex compared with the chloride complex. The secondary bonds between the antimony atom and an iodine ligand from an adjacent $\mathrm{SbI_3}$ unit form asymmetric, weakly associated $\mathrm{Sb_2I_6S_4}$ edge-shared bioctahedra which serve to create a one-dimensional chain. Within this polymeric structure each antimony atom is in a distorted octahedral environment, coordinated to two mutually *cis* sulfur donor atoms from different μ-bridging thioether ligands, two terminal iodine ligands and two μ-bridging iodine atoms. The bridging unit is asymmetric, with bond lengths indicative of primary Sb–I bonds [2.861(2) Å] and secondary Sb–I bonds [3.516(2) Å]. The Sb–S distances [Sb–S(1) 3.021(6), Sb–S(2) 2.973(6) Å] are comparable to those discussed earlier.

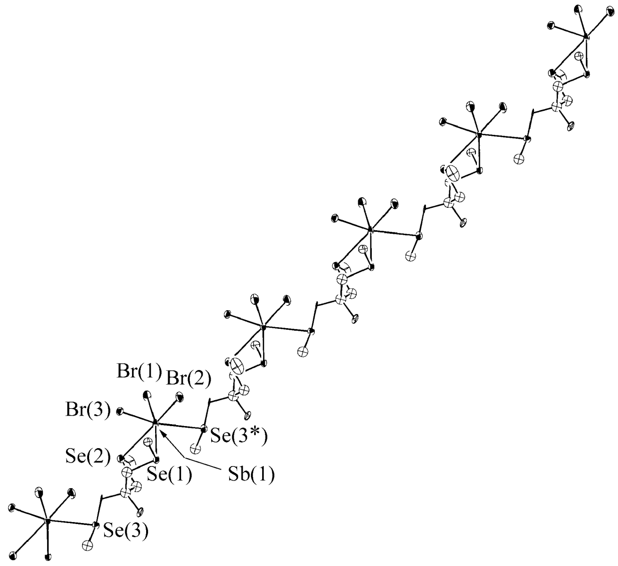

Fig. 5 View of part of the chain structure of [$\mathrm{SbBr_3\{MeC(CH_2SeMe)_3\}}$] with numbering scheme adopted. Atoms marked (*) are related by $\frac{1}{2}+x, \frac{1}{2}-y, \frac{1}{2}+z$. Ellipsoids are drawn at the 40% probability level and H atoms are omitted for clarity.

Table 5 Selected bond lengths (Å) and angles (°) for [$\mathrm{SbBr_3\{MeC(CH_2SeMe)_3\}}$]

Sb(1)–Br(1)	2.625(4)	Sb(1)–Se(1)	3.162(3)
Sb(1)–Br(2)	2.574(4)	Sb(1)–Se(2)	3.188(4)
Sb(1)–Br(3)	2.580(3)	Sb(1)–Se(3*)	3.195(4)

Br(1)–Sb(1)–Br(2)	98.47(12)	Br(1)–Sb(1)–Br(3)	90.94(11)
Br(1)–Sb(1)–Se(1)	168.70(12)	Br(1)–Sb(1)–Se(2)	91.30(11)
Br(1)–Sb(1)–Se(3*)	85.78(10)	Br(2)–Sb(1)–Br(3)	91.20(12)
Br(2)–Sb(1)–Se(1)	90.57(11)	Br(2)–Sb(1)–Se(2)	166.70(12)
Br(2)–Sb(1)–Se(3*)	77.88(11)	Br(3)–Sb(1)–Se(1)	82.06(9)
Br(3)–Sb(1)–Se(2)	79.57(10)	Br(3)–Sb(1)–Se(3*)	167.98(10)
Se(1)–Sb(1)–Se(2)	78.76(9)	Se(1)–Sb(1)–Se(3*)	102.83(9)
Se(2)–Sb(1)–Se(3*)	112.03(9)		

The bond angles S(1)–Sb(1)–I(2) [174.0(1)°], I(3)–Sb(1)–I(1*) [177.39(7)°] and I(1)–Sb(1)–I(1*) [85.05(6)°] indicate that the geometry about the antimony(III) atom is distorted from an idealised octahedron. The structure of this species is rather similar to that of [$\mathrm{SbCl_3\{MeSe(CH_2)_3SeMe\}}$].[4]

Other than the species recently communicated by us,[4] there are no structurally characterised examples of antimony(III) selenoether compounds. The structure of [$\mathrm{SbBr_3\{MeC(CH_2SeMe)_3\}}$] shows six coordinate Sb(III) centres, which adopt distorted octahedral environments, giving an infinite one-dimensional coordination polymer (Fig. 5, Table 5). The coordination set comprises three terminal Br and a *fac*-coordinated set of three Se-donors; from one bidentate selenoether and one monodentate selenoether. The Sb–Br bond lengths are once again indicative of primary interactions [Sb–Br(1), Sb–Br(2) and Sb–Br(3), 2.625(4), 2.574(4) and 2.580(3) Å respectively] and bear a close resemblance to the Sb–Br bond lengths in other Sb(III) bromo complexes with Group 16 donor ligands. The three secondary Sb–Se distances are very similar. It is interesting to contrast this structure with that of [$\mathrm{SbCl_3\{MeC(CH_2SMe)_3\}}$] above, which we have chosen to describe as essentially five coordinate, since the third $\mathrm{Sb\cdots S}$ contact is very much longer than the other two.

The structure of [$\mathrm{SbBr_3\{MeC(CH_2SeMe)_3\}}$] compares with the two-dimensional array observed for [$\mathrm{BiCl_3\{MeC(CH_2SeMe)_3\}}$],[2] in which each Bi(III) atom is coordinated to a donor set which includes one bidentate and one monodentate selenoether ligand which bond in a manner similar to the one observed in $[SbBr_3\{MeC(CH_2SeMe)_3\}]$ *i.e.*, the ligand links one metal centre to its neighbour. However, the absence of bridging halides in the antimony species prevents formation of a two-dimensional array like that seen for the bismuth species.

It is noteworthy that all of the structurally characterised Sb(III) complexes reported here repeat infinitely along one-, two- or three-dimensions, with no discrete dimers or capped species identified. This contrasts with the earlier reports on the face-capping discrete monomeric species involving Sb(III) and Bi(III) with thiacrowns. Additionally, the coordinated S or Se atoms lie mutually *cis* in all of the Sb complexes, whereas examples of both *cis* and *trans* dispositions have been identified for analogous Bi systems, *e.g.* $[BiCl_3([8]aneSe_2)]$ and $[BiBr_3([16]aneSe_4)]$.[3]

This work represents the first detailed investigation of antimony(III) halide complexes of acyclic and macrocyclic thio- and seleno-ether ligands. Although the stoichiometry of the products obtained from these reactions has been established beyond doubt, by the very nature of these polymeric antimony(III) species their characterisation is restricted to analytical data, IR spectroscopy and single crystal X-ray diffraction studies. UV-Visible spectroscopy shows that the colours of the complexes arise from ill-defined charge transfer transitions which tail into the visible region. The structural motifs described here represent those species which yielded suitable quality crystals. Other motifs may be obtainable under different conditions. All of the structures which we have identified for these systems are consistent with the bonding model proposed for phosphine complexes of Sb(III) and Bi(III).[16] Essentially the structures are assembled from primary Sb–X interactions and weaker, secondary interactions with the Group 16 donor atoms, probably utilising Sb–X σ^* as the acceptor orbitals. It is difficult to comment on the stereochemical activity (or otherwise) of the Sb-based lone pair. The structures are distorted, but this may be a consequence of the geometrical requirements of the polymeric arrays.

Experimental

Infrared spectra were measured as Nujol mulls between CsI plates using a Perkin-Elmer 983 spectrometer over the range 220–4000 cm^{-1}. ^1H NMR spectra in $CDCl_3$ using a Bruker AM300 spectrometer operating at 300 MHz. Microanalyses were obtained from the University of Strathclyde Microanalytical Laboratory. Antimony trihalides (Aldrich or Alfa) were obtained commercially and used as received. Chalcogenoether ligands were prepared using literature methods,[17–19] except $[12]aneS_4$, $[14]aneS_4$ and $[16]aneS_4$, which were obtained commercially (Aldrich). Standard Schlenk techniques and anhydrous solvents were used for all preparations.

Preparations

$[SbCl_3\{MeS(CH_2)_2SMe\}]$. A solution of $MeS(CH_2)_2SMe$ (0.12 g, 1 mmol) in MeCN (3 cm^3) was added to a stirred and chilled solution of $SbCl_3$ (0.22 g, 1 mmol) in MeCN (10 cm^3). The resultant clear, colourless solution was stirred in an ice bath for 10 min., then in a water bath at 50 °C and then stirred at room temperature overnight. Solvent volume was reduced and the residue layered with *n*-hexane to produce a crop of clear, colourless block crystals suitable for X-ray diffraction studies. Yield 0.28 g, 80%. Required for $C_4H_{10}Cl_3S_2Sb$: C, 13.7; H, 2.9. Found: C, 13.8; H, 2.9%. ^1H NMR: δ 2.2 (s, 6H), 2.8 (s, 4H). IR/cm^{-1}: 270, 243.

$[SbBr_3\{MeS(CH_2)_2SMe\}]$. Procedure as above, using $SbBr_3$ and $MeS(CH_2)_2SMe$. Pale yellow powder. Yield 31%. Required for $C_4H_{10}Br_3S_2Sb$: C, 9.9; H, 2.0. Found: C, 9.7; H, 2.0%. ^1H NMR: δ 2.3 (s, 6H), 2.9 (s, 4H).

$[SbI_3\{MeS(CH_2)_2SMe\}]$. To a chilled and stirred solution of SbI_3 (0.3 g, 0.6 mmol) in thf (10 cm^3) was added a solution of $MeS(CH_2)_2SMe$ (0.074 g, 0.6 mmol) in thf (5 cm^3). The yellow-orange solution was stirred at room temperature for 1 hour and solvent removed *in vacuo* to produce an orange powder, which was washed with CH_2Cl_2 and dried *in vacuo*. Orange powder. Yield 68%. Required for $C_4H_{10}I_3S_2Sb$: C, 7.7; H, 1.6. Found: C, 7.9; H, 1.2%. ^1H NMR: δ 2.2 (s, 6H), 2.7 (s, 4H).

$[SbCl_3\{MeS(CH_2)_3SMe\}]$. Procedure as for $[SbCl_3\{MeS(CH_2)_2SMe\}]$ above, using $SbCl_3$ and $MeS(CH_2)_3SMe$. Off-white powder. Yield 67%. Required for $C_5H_{12}Cl_3S_2Sb$: C, 16.5; H, 3.3. Found: C, 16.2; H, 3.2%. ^1H NMR: δ 1.9 (q, 2H), 2.1 (s, 6H), 2.6 (t, 4H). IR/cm^{-1}: 254, 235.

$[SbBr_3\{MeS(CH_2)_3SMe\}]$. Procedure as above, using $SbBr_3$ and $MeS(CH_2)_3SMe$. White solid. Yield 51%. Required for $C_5H_{12}Br_3S_3Sb$: C, 12.1; H, 2.4. Found: C, 12.6; H, 2.4%. ^1H NMR: δ 1.9 (q, 2H), 2.1 (s, 6H), 2.6 (t, 4H).

$[SbBr_3\{MeSe(CH_2)_2SeMe\}]$. As above, using $SbBr_3$ and $MeSe(CH_2)_2SeMe$. Pale yellow solid. Yield 31%. Required for $C_4H_{10}Br_3SbSe_2$: C, 8.3; H, 1.8. Found: C, 8.8; H, 1.9%.

$[SbI_3\{MeSe(CH_2)_2SeMe\}]$. As above, using SbI_3 and $MeSe(CH_2)_2SeMe$. Orange powder. Yield 82%. Required for $C_4H_{10}I_3SbSe_2$: C, 6.7; H, 1.4. Found: C, 6.3; H, 1.3%. ^1H NMR: δ 2.1 (s, 6H), 2.9 (s, 4H).

$[SbCl_3([12]aneS_4)]$. To an MeCN solution of $SbCl_3$ (0.048 g, 0.21 mmol) was added an equimolar MeCN solution of $[12]aneS_4$ (0.050 g, 0.21 mmol). The clear, colourless solution was stirred briefly at room temperature and solvent removed *in vacuo* to leave an off-white powder. Yield 63%. Required for $C_8H_{16}Cl_3S_4Sb$: C, 20.5; H, 3.4. Found: C, 21.0; H, 3.5%. IR/cm^{-1}: 253, 244, 230.

$[SbBr_3([12]aneS_4)]$. Procedure as above, using $SbBr_3$ and $[12]aneS_4$. Pale yellow powder. Yield 57%. Required for $C_8H_{16}Br_3S_4Sb$: C, 16.0; H, 2.7. Found: C, 16.5; H, 2.6%.

$[SbCl_3([14]aneS_4)]$. Procedure as above, using $SbCl_3$ and $[14]aneS_4$. White powder. Yield 35%. Required for $C_{10}H_{20}Cl_3S_4Sb$: C, 24.2; H, 4.0. Found: C, 23.8; H, 3.9%. IR/cm^{-1}: 267, 249, 231.

$[(SbBr_3)_2([14]aneS_4)]$. Procedure as above, using $SbBr_3$ and $[14]aneS_4$. Pale yellow crystals. Yield 40%. Required for $C_{10}H_{20}Br_6S_4Sb_2\cdot MeCN$: C, 14.0; H, 2.2. Found: C, 14.1; H, 2.3%.

$[SbCl_3([16]aneS_4)]$. Procedure as above, using $SbCl_3$ and $[16]aneS_4$. White powder. Yield 30%. Required for $C_{12}H_{24}Cl_3S_4Sb$: C, 27.5; H, 4.6. Found: C, 27.2; H, 4.3%. IR/cm^{-1}: 253, 241, 231.

$[SbBr_3([16]aneS_4)]$. Procedure as above, using $SbBr_3$ and $[16]aneS_4$. Pale yellow powder. Yield 35%. Required for $C_{12}H_{24}Br_3S_4Sb$: C, 21.9; H, 3.7. Found: C, 21.8; H, 3.6%.

$[SbCl_3\{MeC(CH_2SMe)_3\}]$. An ice cold solution of $SbCl_3$ (0.20 g, 0.88 mmol) in MeCN (10 cm^3) was treated dropwise with $MeC(CH_2SMe)_3$ (0.18 g, 0.88 mmol) under an atmosphere of N_2. The solvent was slowly removed *in vacuo* to give a white, microcrystalline solid. Yield 0.23 g, 60%. Required for $C_8H_{18}Cl_3S_3Sb$: C, 21.9; H, 4.2. Found: C, 22.0; H, 4.3%. IR/cm^{-1}: 327, 290.

$[SbBr_3\{MeC(CH_2SMe)_3\}]$. As above, using $SbBr_3$ and $MeC(CH_2SMe)_3$. Yellow powder. Yield 40%. Required for $C_8H_{18}Br_3S_3Sb$: C, 16.8; H, 3.5. Found: C, 16.5; H, 3.0%.

Table 6 Crystallographic data.

	[SbCl$_3${MeS(CH$_2$)$_2$SMe}]	[SbCl$_3${MeC(CH$_2$SMe)$_3$}]	[SbI$_3${MeC(CH$_2$SMe)$_3$}]	[SbBr$_3${MeC(CH$_2$SeMe)$_3$}]	[(SbBr$_3$)$_2$([14]aneS$_4$)]
Formula	$C_4H_{10}Cl_3S_2Sb$	$C_8H_{18}Cl_3S_3Sb$	$C_8H_{18}I_3S_3Sb$	$C_8H_{18}Br_3SbSe_3$	$C_{10}H_{20}Br_6S_4Sb_2$
M	350.35	438.52	712.87	712.57	991.43
Crystal system	Orthorhombic	Orthorhombic	Triclinic	Monoclinic	Monoclinic
Space group	$P2_12_12_1$	$P2_12_12_1$	$P\bar{1}$	Cc	$P2_1/n$
a/Å	8.925(3)	9.479(1)	11.198(7)	11.9999(3)	6.897(6)
b/Å	15.098(2)	18.736(1)	12.017(8)	15.2832(4)	13.30(1)
c/Å	8.224(3)	9.056(2)	7.584(3)	9.9029(3)	13.78(1)
α/°			93.98(5)		
β/°			98.28(5)	104.477(1)	103.27(7)
γ/°			114.44(5)		
U/Å^3	1108.2(4)	1608.4(3)	910(1)	1758.49(8)	1230(2)
Z	4	4	2	4	2
μ(Mo-Kα)/cm^{-1}	35.22	25.72	68.74	145.9	123.02
Unique obs. reflections	1169	1669	3194	2095	4314
Obs. reflections with [$I > 2\sigma(I)$]	1093	1495	2786	1281	3040
R	0.028	0.024	0.081	0.063	0.065
Rw	0.029	0.027	0.122	0.068	0.072

[SbI$_3${MeC(CH$_2$SMe)$_3$}]. As above, using SbI$_3$ and MeC(CH$_2$SMe)$_3$. Yellow-orange powder. Yield 52%. Required for $C_8H_{18}I_3S_3Sb$: C, 13.5; H, 2.5. Found: C, 13.2; H, 2.6%.

[SbCl$_3${MeC(CH$_2$SeMe)$_3$}]. As above, using SbCl$_3$ and MeC(CH$_2$SeMe)$_3$. Cream coloured powder. Yield 60%. Required for $C_8H_{18}Cl_3SbSe_3$: C, 16.6; H, 3.1. Found: C, 16.8; H, 2.9%. IR/cm^{-1}: 290, 252.

[SbBr$_3${MeC(CH$_2$SeMe)$_3$}]. As above, using SbBr$_3$ and MeC(CH$_2$SeMe)$_3$. Yellow powder. Yield 49%. Required for $C_8H_{18}Br_3SbSe_3$: C, 13.5; H, 2.6. Found: C, 13.0; H, 2.3%.

[SbI$_3${MeC(CH$_2$SeMe)$_3$}]. As above, using SbI$_3$ and MeC(CH$_2$SeMe)$_3$. Orange powder. Yield 59%. Required for $C_8H_{18}I_3SbSe_3$: C, 11.3; H, 2.1. Found: C, 10.8; H, 1.8%.

[SbCl$_3$([8]aneSe$_2$)]. As above, using SbCl$_3$ and [8]aneSe$_2$. Yellow solid. Yield 79%. Required for $C_6H_{12}Cl_3SbSe_2$: C, 15.3; H, 2.6. Found: C, 15.0; H, 2.2%. IR/cm^{-1}: 280 br.

[SbBr$_3$([8]aneSe$_2$)]. As above, using SbBr$_3$ and [8]aneSe$_2$. Orange-red solid. Yield 63%. Required for $C_6H_{12}Br_3SbSe_2$: C, 11.9; H, 2.0. Found: C, 11.6; H, 2.2%.

[SbI$_3$([8]aneSe$_2$)]. As above, using SbI$_3$ and [8]aneSe$_2$. Red solid. Yield 66%. Required for $C_6H_{12}I_3SbSe_2$: C, 9.7; H, 1.6. Found: C, 9.4; H, 1.6%.

[(SbCl$_3$)$_2$([16]aneSe$_4$)]. As above, using SbCl$_3$ and [16]aneSe$_4$. White solid. Yield 35%. Required for $C_{12}H_{24}Cl_6Sb_2Se_4$: C, 15.3; H, 2.6. Found: C, 15.6; H, 3.0%. IR/cm^{-1}: 304, 291.

[(SbI$_3$)$_2$([16]aneSe$_4$)]. As above, using SbI$_3$ and [16]aneSe$_4$. Orange solid. Yield 23%. Required for $C_{12}H_{24}I_6Sb_2Se_4$: C, 9.7; H, 1.6. Found: C, 9.3; H, 1.5%.

X-Ray crystallography

Details of the crystallographic data collection and refinement parameters are given in Table 6. Crystals of [SbCl$_3${MeS(CH$_2$)$_2$SMe}], [(SbBr$_3$)$_2$([14]aneS$_4$)], [SbCl$_3${MeC(CH$_2$SMe)$_3$}], [SbI$_3${MeC(CH$_2$SMe)$_3$}] and [SbBr$_3${MeC(CH$_2$SeMe)$_3$}] were obtained by slow evaporation from a solution of the complex in MeCN. Data collection used a Rigaku AFC7S four-circle diffractometer (or an Enraf Nonius Kappa CCD diffractometer—[SbBr$_3${MeC(CH$_2$SeMe)$_3$}]) ($T = 150$ K) with graphite monochromated Mo-Kα radiation ($\lambda = 0.71073$ Å). The [SbI$_3${MeC(CH$_2$SMe)$_3$}] crystals were not of particulalry high quality, hence giving rise to higher than normal residuals, although the atom connectivities are not in doubt. Otherwise structure solution and refinement were routine.[20–26] Selected bond lengths and angles are presented in Tables 1–5.

CCDC reference numbers 160547–160551.

See http://www.rsc.org/suppdata/dt/b1/b100782n/ for crystallographic data in CIF or other electronic format.

Acknowledgements

We thank the EPSRC for support and Professor M. B. Hursthouse for access to the Nonius Kappa CCD diffractometer.

References

1 A. R. J. Genge, W. Levason and G. Reid, *Chem. Commun.*, 1998, 2159.

2 A. J. Barton, A. R. J. Genge, W. Levason and G. Reid, *J. Chem. Soc., Dalton Trans.*, 2000, 859.

3 A. J. Barton, A. R. J. Genge, W. Levason and G. Reid, *J. Chem. Soc., Dalton Trans.*, 2000, 2163.

4 A. J. Barton, N. J. Hill, W. Levason, B. Patel and G. Reid, *Chem. Commun.*, 2001, 95.

5 E. Hough, D. G. Nicholson and A. K. Vasudevan, *J. Chem. Soc., Dalton Trans.*, 1987, 427.

6 N. W. Alcock, M. Ravindran and G. R. Willey, *Acta Crystallogr., Sect. B*, 1993, **49**, 507.

7 N. W. Alcock, M. Ravindran, S. M. Roe and G. R. Willey, *Inorg. Chim. Acta*, 1990, **167**, 115.

8 A. Lipka, *Acta Crystallogr., Sect. B*, 1979, **35**, 3020.

9 G. R. Willey, D. R. Aris and W. Errington, *Inorg. Chim. Acta*, 2000, **300**, 1004.

10 G. R. Willey, M. T. Lakin, M. Ravindran and N. W. Alcock, *J. Chem. Soc., Chem. Commun.*, 1991, 271.

11 S. Pohl, D. Hasse and M. Peters, *Z. Anorg. Allg. Chem.*, 1993, **619**, 727.

12 M. G. B. Drew, J. M. Kisenyi and G. R. Willey, *J. Chem. Soc., Dalton Trans.*, 1982, 1729.

13 V. M. Schmidt, R. Bender and C. Burschka, *Z. Anorg. Allg. Chem.*, 1979, **454**, 160.

14 T. Bjorvatten, *Acta Chem. Scand.*, 1966, **20**, 1863.

15 G. R. Willey, M. T. Lakin and N. W. Alcock, *J. Chem. Soc., Dalton Trans.*, 1992, 591; G. R. Willey, M. T. Lakin and N. W. Alcock, *J. Chem. Soc., Dalton Trans.*, 1992, 1339.

16 *The Chemistry of Arsenic, Antimony and Bismuth*, ed. N. C. Norman, Blackie, London, 1992.

17 F. R. Hartley, W. Levason, C. A. McAuliffe, S. G. Murray and H. E. Soutter, *Inorg. Chim. Acta*, 1979, **35**, 265; E. G. Hope, T. Kemmitt and W. Levason, *J. Chem. Soc., Perkin Trans. 2*, 1987, 487.

18 R. Ali, S. J. Higgins and W. Levason, *Inorg. Chim. Acta*, 1984, **84**, 65; D. J. Gulliver, E. G. Hope, W. Levason, G. L. Marshall, S. G. Murray and D. M. Potter, *J. Chem. Soc., Perkin Trans. 2*, 1984, 429.

19 R. J. Batchelor, F. W. B. Einstein, I. D. Gay, J. H. Gu, B. D. Johnston and B. M. Pinto, *J. Am. Chem. Soc.*, 1989, **111**, 6582.

20 SHELXS-86: G. M. Sheldrick, *Acta Crystallogr., Sect. A*, 1990, **46**, 467.

21 PATTY, The DIRDIF Program System, P. T. Beurskens, G. Admiraal, G. Beurskens, W. P. Bosman, S. Garcia-Granda, R. O. Gould, J. M. M. Smits and C. Smykalla, Technical Report of the Crystallography Laboratory, University of Nijmegen, The Netherlands, 1992.

22 A. Altomare, M. Cascarano, C. Giocovazzo and A. Guagliardi, *J. Appl. Crystallogr.*, 1993, **26**, 343.

23 TeXsan: Crystal Structure Analysis Package, Molecular Structure Corporation, Texas, 1995.

24 N. Walker and D. Stuart, *Acta Crystallogr., Sect. A*, 1983, **39**, 158.

25 H. D. Flack, *Acta Crystallogr., Sect. A*, 1983, **39**, 876.

26 R. H. Blessing, *Acta Crystallogr., Sect. A*, 1995, **51**, 33; R. H. Blessing, *J. Appl. Crystallogr.*, 1997, **30**, 421.